

Facile synthesis of organo-soluble surface-grafted all-single-layer graphene oxide as hole-injecting buffer material in organic light-emitting diodes†

Ze Zhong, Yanfeng Dai, Dongge Ma and Zhi Yuan Wang*

Received 5th January 2011, Accepted 16th February 2011

DOI: 10.1039/c1jm00044f

Graphene oxide (GO) was modified by surface grafting and the product P-GO exhibited a surprisingly good solubility in common solvents (as high as 1.8 mg mL^{-1} in DMF) without sonication and can be spin coated to form large single-layer sheets on a substrate. In contrast to GO, all-single-layer P-GO sheets are readily formed in solution, which are highly useful for separation from other multi-layer sheets and as precursors to all-single-layer graphene. The unique property of single-layer P-GO made it a promising functional material, such as hole-injecting buffer (HIB) material in organic light-emitting devices. The devices using P-GO as a hole-injecting buffer layer on the ITO electrode perform better than those with PEDOT:PSS.

1. Introduction

The injection of charge carriers from electrodes into organic layers is an extremely important process in organic devices, such as organic light emitting diodes (OLEDs) and photovoltaic devices. In the devices using indium tin oxide (ITO) as an anode, a large hole-injection barrier is often found at the ITO/organic interface because the work function of ITO is in the range of 4.1–4.7 eV, which is significantly lower than the typical ionization energy of organic materials.¹ Electrically doped charge transport layers may be used to enhance the injection of charge carriers from an ITO anode into organic layers,² such as the use of a strong electron acceptor F4-TCNQ in the hole transport layer³ and the use of poly(3,4-ethylenedioxythiophene):poly(styrenesulfonate) (PEDOT:PSS) on top of the ITO electrode.⁴ The PEDOT:PSS dispersion is considered today to be the most promising and most widely used hole-injecting buffer (HIB) material in OLED research and development. Furthermore, the PEDOT:PSS layer acts as a physical barrier against the many defect sites known to be present in ITO. However, due to its high acidity, PEDOT:PSS can gradually erode the ITO electrode over time, making it necessary to explore other organic HIB materials. Among the reported anodic buffer layers, a large number of transition metal oxides, such as V_2O_5 ,⁵ MoO_x ,⁶ WO_3 ,⁷ CuO_x ,⁸ NiO ,⁹ and Fe_3O_4 ,¹⁰ have been used to lower the hole-

injection barrier and improve the interface morphology. In comparison, solution-processable organic hole-injecting buffer material that can replace PEDOT:PSS is desirable but scarce.

The water-soluble graphene oxide (GO) is often used as a precursor for graphene,^{11–14} and also shows a great potential for use in optoelectronic devices such as organic solar cells.¹⁵ However, a small amount of water that is tightly adsorbed on GO can adversely affect the performance of OLEDs and other organic optoelectronic devices, such as the formation of dark spots and pixel shrinkage over time due to intrusion of water and air. In addition, the water-soluble GO is made with the layer numbers beyond control and tends to form multilayered sheets, which may hamper its ability as an anodic buffer material since similar to graphene the property of GO is also dependent on the layer number of the sheets.^{16–18} Therefore, structural modification of GO is needed to improve its solubility in anhydrous organic solvents and make it available as all-single-layer sheets with the desirable and fairly consistent electrical property for use in OLEDs and other organic devices. Accordingly, by reducing interaction between GO sheets, surface grafting with long-chain molecules is deemed necessary and appropriate in order to obtain single-layer GO sheets with a good solubility in organic solvents.

2. Experimental**Materials**

4-Aminophenol, Aliquat® 336 and 1-chlorooctane were received from Aladdin Reagent Company. All the solvents were purchased from Beijing Chemical Company and were used without purification.

State Key Laboratory of Polymer Physics and Chemistry, Changchun Institute of Applied Chemistry, Chinese Academy of Sciences and Graduate School of Chinese Academy of Sciences, Changchun, 130022, China. E-mail: wwjoy@ciac.jl.cn; Fax: +86 431 852901; Tel: +86 431 85262901

† Electronic supplementary information (ESI) available: Pyrolysis-GC/MS of P-GO; IR spectra of graphite oxide and P-GO; Raman spectrum of P-GO; TEM image of P-GO sheets; XRD spectrum of graphite oxide; AFM images of chemically reduced graphene. See DOI: 10.1039/c1jm00044f

Synthesis of 4-(octoxy)aniline^{19,20}

To a 100 mL flask were added 4-aminophenol (20 mmol, 2.18 g), 1-chlorooctane (20 mmol, 2.98 g), NaOH (40 mmol, 2.76 g) and Aliquat® 336 (1.0 mmol, 0.404 g). The mixture was stirred in Ar at 60 °C for 15 h. The dark brown mixture was diluted with dichloromethane, filtered and then washed with deionized water three times. The organic phase was dried over Na₂SO₄, concentrated in vacuum to give dark brown oily residue. The crude product was purified by chromatography (silica gel, ethyl acetate/petroleum ether (60–90 °C) = 1/3 as the eluent). The product was a light brown solid (4.90 g, 77% yield). ¹H NMR (300 MHz, CDCl₃): δ 6.63–6.76 (m, 4H), 3.87 (t, *J* = 6.61 Hz, 2H), 1.71–1.76 (m, 2H), 1.20–1.40 (m, 12H), 0.84–0.90 (m, 3H).

Synthesis of 4-(octoxy)benzenediazonium tetrafluoroborate^{21,22}

A flask charged with 4-(octoxy)aniline (10 mmol, 3.20 g) and HCl solution (1 : 1, 6 mL) was heated and then cooled in an ice-bath for 10 min. A solution of NaNO₂ (2 mol L⁻¹, 0.70 g of NaNO₂) was added dropwise. The mixture was then stirred for 1 h, followed by addition of the saturated solution of NaBF₄ (1.7 g). The resulting mixture was stirred for another 30 min in an ice-bath, filtered, and washed with deionized water and cold methanol to give light powder (2.27 g, 71% yield). ¹H NMR (300 MHz, CDCl₃) δ 8.51–8.59 (d, 2H), 7.16–7.23 (d, 2H), 4.15–4.23 (t, 2H), 1.23–1.51 (10H), 0.84–0.94 (m, 3H).

Synthesis of graphite oxide

Graphite oxide was synthesized using a modified procedure of Hummers and Offeman.²³ Graphite (1.0 g, Alfa Aesar, 325 mesh) and NaNO₃ (1.5 g) and concentrated sulfuric acid (25 mL) were charged to a 250 mL flask that was placed in an ice bath, followed by addition of KMnO₄ (4.5 g) slowly. The mixture was allowed to warm up to 35 °C for 30 min and then stirred at room temperature for another 2 h. The brownish grey paste was then diluted with deionized water (500 mL) with caution. The suspension was then further diluted to a total volume of 1.5 L with deionized water and H₂O₂ (5 mL, 30%) and then filtered. The brown cake was dispersed in a solution of 3 wt% H₂SO₄/0.5 wt% H₂O₂ (200 mL) and then filtered. This washing process was repeated for 5 times and the product was washed with deionized water repeatedly until the filtrate was pH 7. After drying in vacuum at 50 °C for 5 h, GO was obtained as brown powder (1.6 g).

Preparation of P-GO

Aqueous solution of as-prepared GO (1 mg mL⁻¹, 60 mL) was sonicated and then reacted with 4-octoxyphenyldiazonium tetrafluoroborate at room temperature for a given time (*e.g.*, 10–60 min). The suspension was filtered through a PTFE membrane (0.45 μm), copiously washed with acetone and DMF, and dried in vacuum at 60 °C for 5 h to yield P-GO (70–90 mg).

Device fabrication and measurement

The OLEDs were fabricated by thermal vacuum deposition on prepatterned ITO-coated glass substrates with sheet resistances of 10 ohms per square. The substrate was ultrasonically cleaned

with acetone (2 times), detergent, deionized water (2 times), and ethanol (2 times) in sequence, followed by oxygen-plasma cleaning. The thermal evaporation of organic materials was carried out at a chamber pressure of 10⁻⁴ Pa. The thickness of each layer was determined by a quartz thickness monitor. PEDOT:PSS was spin-coated on ITO-coated glass at the speed of 3000 rpm for 60 s and then dried at 120 °C in vacuum for 1 h. P-GO was spin-coated on ITO-coated glass at the speed of 3000 rpm for 30 s and then dried at 80 °C for 1 h. The effective size of the light-emitting diode was 16 mm².

Current–voltage–power measurements were performed simultaneously using a Keithley 2400 Source meter and a Newport 1830-C Optical meter equipped with a Newport 818-UV silicon photodiode, respectively. All the measurements were carried out under ambient atmosphere at room temperature.

Characterization

XRD measurements were performed using a Philips PW1700 X-ray diffractometer. TEM images were recorded on a JEM-1011 transmission electron microscope. AFM images were obtained using SPI3800N probe station and SPA400SPM. Infrared spectra were collected on a Shimadzu IRAffinity-1 in an attenuated total reflectance (ATR) mode. Thermogravimetry measurements were recorded using a Perkin-Elmer-TGA 7. Raman spectra were collected on a Horiba LabRAM HR 800 Raman spectrometer. Pyrolysis-GC/MS data were obtained using a CDS 5000 with an Agilent 5975 GC/MS.

3. Results and discussion

Graphene oxide can be readily modified by either covalent^{24–27} or non-covalent^{28–31} bonding methods. By covalent bonding through the carboxylic acid groups *via* the esterification or acylation reactions, the degree of functionalization is dependent on the number of the carboxylic acid groups available at the edges of GO sheets and is too low to impart a meaningful solubility to the modified GO. In addition to functionalization on the edges, a single-layer GO sheet has two surfaces accessible to chemical modification. The surface grafting with a large number of long-chain molecules can be expected to effectively diminish the van der Waals force between the GO sheets, which should improve the solubility in organic solvents. For bi-layer and multi-layer GO sheets, since only the edges and both sides are available for functionalization, the resulting products would have a lower solubility than single-layer GO sheets.

In our work, freshly prepared GO was simply treated with 4-octoxyphenyldiazonium tetrafluoroborate at room temperature for 10 to 60 min to yield the phenylated graphene oxide (P-GO), similar to a reaction of graphene or expanded graphite with aryldiazonium salts.³² The solubility of P-GO is very much dependent on the degree of functionalization or reaction time. The higher the solubility is, the higher the degree of grafting or functionalization of GO should be. The number of octoxyphenyl groups that can be introduced into GO seems to reach a maximum after 60 minutes of the reaction, which gives rise to P-GO (sample C) with the highest solubility of 1.8 mg mL⁻¹ in DMF ever reported to date. At the reaction time of 10 min and 30 min, the two different P-GO samples (A and B) were obtained

with a solubility of 0.6 mg mL^{-1} in DMF for sample A and 1.0 mg mL^{-1} for sample B, respectively.

It was found that all the P-GO samples can be dissolved in DMF with only gentle stirring at room temperature, without aid of sonication or surfactant and ionic liquid, and the solution is stable for more than 2 months without any precipitation. It is known that sonication over a long time may break up and crumb GO sheets to small particles, which would adversely affect the device performance. Thus, high solubility of P-GO offers a better chance to obtain and maintain the large-size GO sheets. To ensure the reproducibility, the starting GO was prepared under the same conditions from batch to batch. As a result, the P-GO produced in each batch showed similar characteristics and properties.

The success of the grafting reaction or the presence of the octoxyphenyl groups in P-GO was first confirmed by thermogravimetric analysis. Thermogravimetry (TG) in nitrogen atmosphere was performed up to $800 \text{ }^\circ\text{C}$ on P-GO samples (A and B) and the parent graphite oxide for comparison. The weight loss of graphite oxide is $\sim 57\%$ at $800 \text{ }^\circ\text{C}$ (trace C, Fig. 1), similar to the reported value,^{24,33,34} and is less than the overall weight loss of P-GO samples A (62%) and B (68%). The extra weight loss from P-GO is clearly attributed to the presence of the octoxyphenyl groups, since it is reasonable to believe no residual octoxyphenyl groups are still attached to GO at this high temperature. Accordingly, P-GO samples A and B contain $\sim 13\%$ and $\sim 34\%$ of the octoxyphenyl groups. The initial weight loss below $150 \text{ }^\circ\text{C}$ is due to adsorbed water or DMF in three samples. P-GO was further characterized by pyrolysis-GC/MS at $250 \text{ }^\circ\text{C}$, which confirms the presence of the octoxyphenyl groups in P-GO (Fig. S1 in the ESI†).

The P-GO samples were then characterized by IR in comparison with graphite oxide (Fig. S2 in the ESI†). The new peaks at 1248 and 1105 cm^{-1} are assigned to the ether moiety of the octoxyphenyl groups. The Raman spectrum (633 nm laser excitation) of P-GO sample B (Fig. S3 in the ESI†) displays two bands at 1327 and 1573 cm^{-1} corresponding to the D (disorder band) and G (in-phase vibration) bands, respectively. The D-band indicates a large disorder caused by unreduced oxygen groups in GO and introduction of the aryl groups. The weak 2D

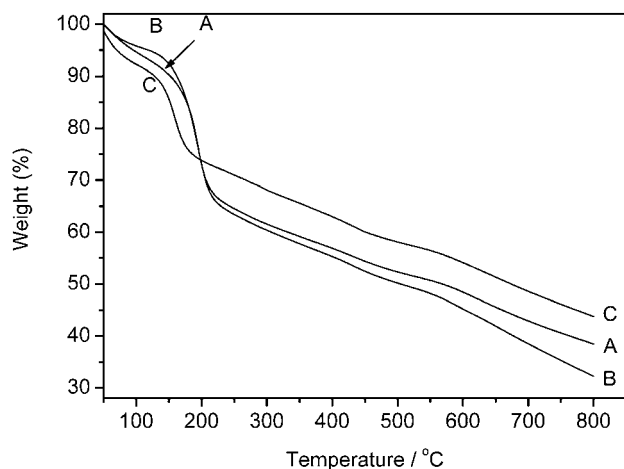


Fig. 1 Thermogravimetric traces of P-GO sample A (trace A), sample B (trace B) and graphite oxide (trace C) in nitrogen.

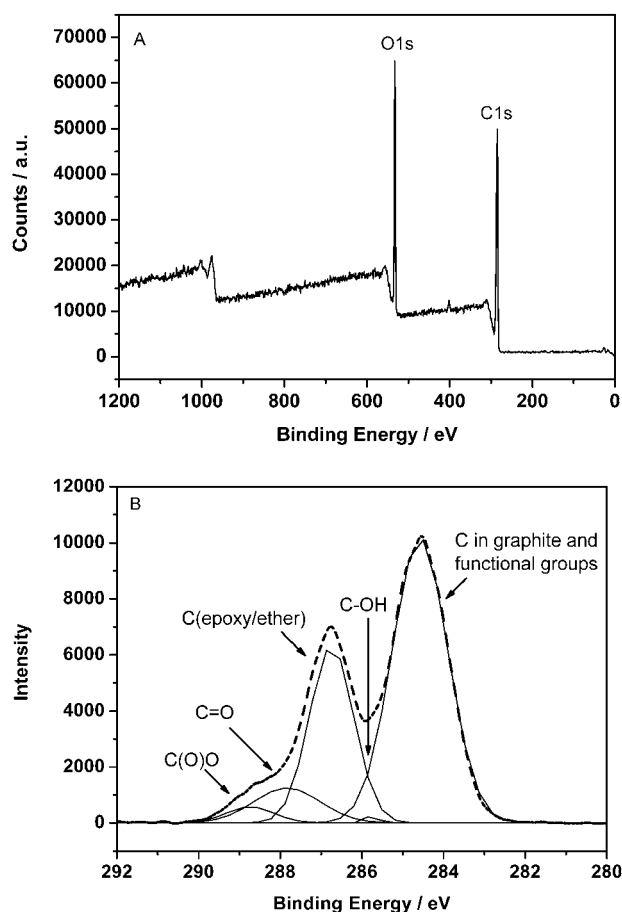


Fig. 2 (A) Survey XPS spectrum and (B) deconvoluted C1s spectrum (lines) of P-GO sample B.

band at $\sim 2640 \text{ cm}^{-1}$ is indicative of the sp^2 network in P-GO. The peaks shift to lower frequency because of lower incident laser excitation energy and the substrate effect.^{35–39}

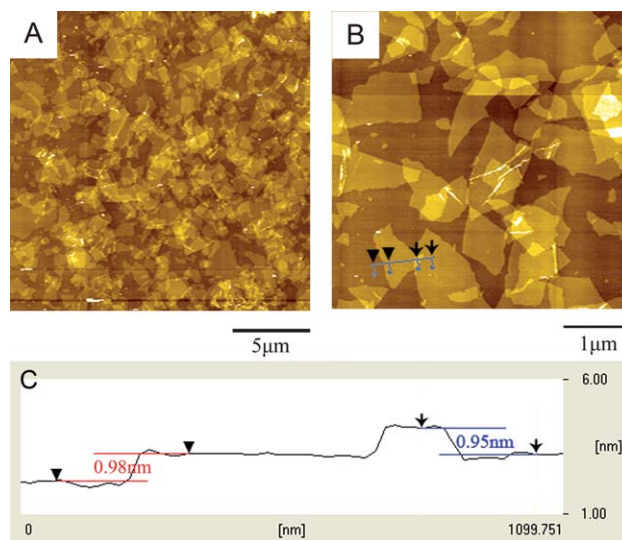


Fig. 3 AFM images of P-GO (sample B) films spin-coated on freshly cleaved mica. (A) $20 \times 20 \text{ } \mu\text{m}$, (B) $5 \times 5 \text{ } \mu\text{m}$, (C) height profile of P-GO sheets in (B).

Finally, the composition of P-GO was analyzed by X-ray photoelectron spectroscopy (XPS). As shown in Fig. 2, the high intensity of O1s is due to the residual oxygen from GO together with oxygen from the octoxyphenyl moiety. The deconvoluted C1s spectrum (Fig. 2B) shows various types of carbons, which represents various functional groups in P-GO.⁴⁰

The films of P-GO readily form on various substrates (*e.g.*, glass, mica and ITO) by spin-coating of its solution in DMF. The topography of P-GO film (sample B) cast from the DMF solution with a concentration of 1.0 mg mL⁻¹ on freshly cleaved mica

was imaged by AFM using a tapping mode (Fig. 3). The height of all the films is between 0.8 and 1.2 nm and falls in an acceptable height range for modified single-layer graphene.^{16,41,42} Therefore, the spin-coated P-GO films are all-single-layer sheets. The AFM images further indicate that the size of the all-single-layer P-GO sheets is up to 1 μm and the average R_a of the P-GO film over an area of 20 \times 20 μm^2 is *ca.* 0.81 nm. The morphology of the P-GO sheets was further revealed by transmission electron microscopy (TEM) to be highly transparent, largely stacked and wrinkled (Fig. S4 in the ESI[†]). The XRD spectrum of graphite oxide

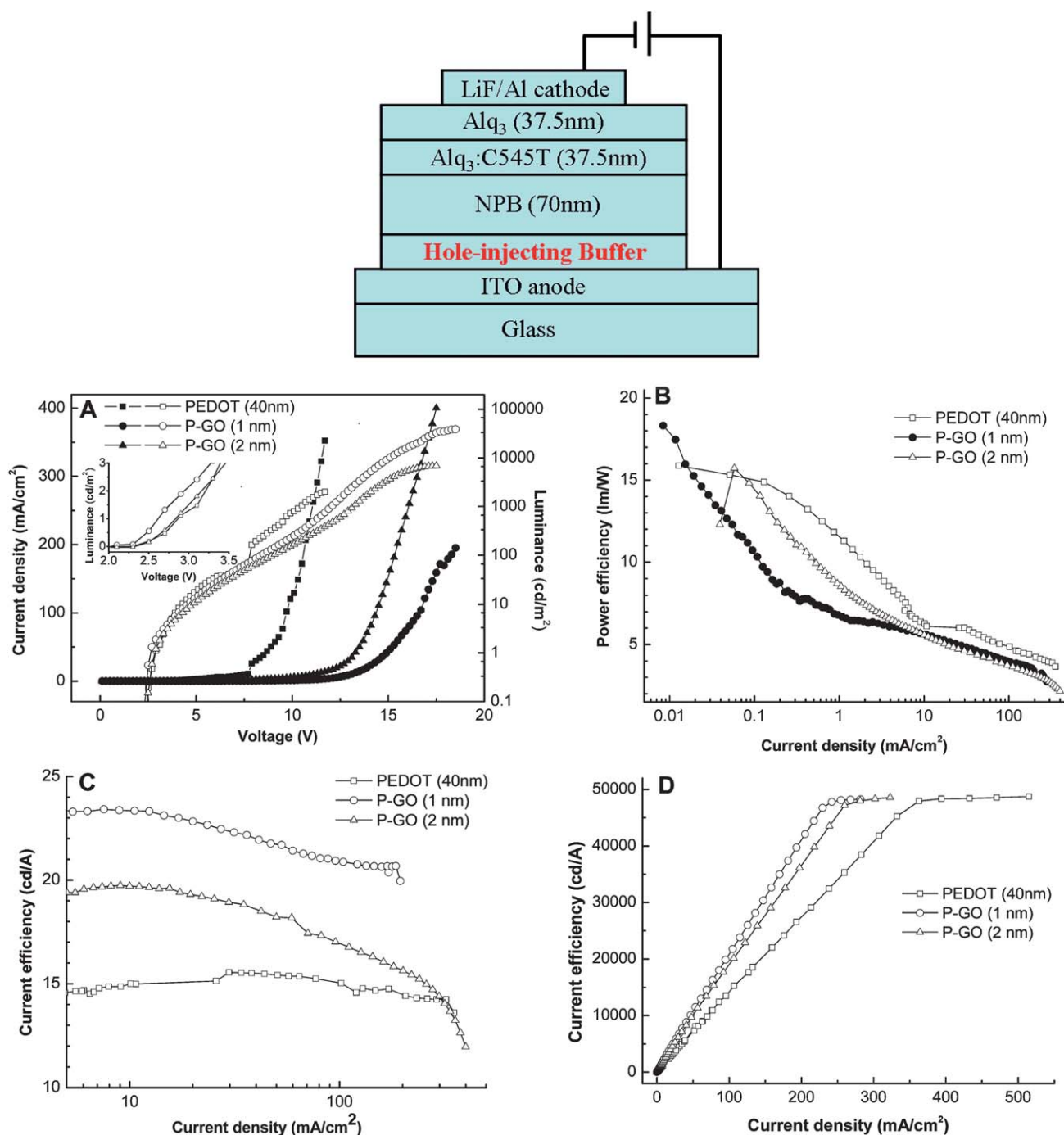


Fig. 4 Structure of the OLED device. (A) The C - V - L characteristics of OLED with the P-GO layer (sample B) as a hole-injecting buffer layer. (B) Power efficiency. (C) Current efficiency. (D) Luminance.

(Fig. S5 in the ESI†) displays a peak at 10.2° and the interlayer spacing is calculated to be 8.66 Å. However, there is no peak or layered structures for P-GO, which implies the single-layer P-GO sheets. Therefore, the surface grafting imparts high solubility and low interaction to graphene oxide, which in turn promotes the formation of large-area and single-layer sheets.

Since single-layer P-GO sheets are readily formed, subsequent reduction is expected to afford single-layer graphene sheets. Thus, the spin-coated P-GO films on freshly cleaved mica were reduced with hydrazine hydrate vapor. The change in the chemical structure after reduction is evident by the changes in the IR spectra (1000–1500 cm⁻¹, Fig. S2†). By AFM analysis, the average height of as-prepared graphene sheets was in a range of 0.6–0.9 nm (Fig. S6 in the ESI†), which significantly decreased from the original height of 0.8–1.2 nm for the P-GO films, strongly suggesting the formation of single-layer graphene.

P-GO is an insulator because of the disrupted sp² conjugation of the graphene lattice. However, the residual sp² clusters in P-GO can still allow for hole or electron transport to occur at the Fermi level by hopping. Taking a fairly large resistance of P-GO into account, it is conceivable to use P-GO as a HIB layer in OLEDs. Accordingly, the green light-emitting diodes were fabricated using DMF-soluble P-GO samples, in order to investigate its usefulness as an alternative to PEDOT and the structural effect that the P-GO sheets may have due to a different degree of surface grafting on the device performance. The four OLED devices having three P-GO samples with different solubilities (0.6, 1.0, and 1.8 mg mL⁻¹ in DMF) and PEDOT:PSS as a HIB were fabricated, all with a device configuration of ITO/HIB/NPB (70 nm)/(Alq₃):C545T (1:0.8 wt%, 37.5 nm)/Alq₃ (37.5 nm)/LiF (1 nm)/Al (100 nm) (Fig. 4), where NPB is 1,4-bis[(1-naphthylphenyl)amino]biphenyl, Alq₃ is tris(8-hydroxyquinolinato)aluminium and C545T is 10-(2-benzothiazolyl)-2,3,6,7-tetrahydro-1,1,7,7-tetramethyl-1*H*,5*H*,11*H*-(1)benzopyrroprano(6,7-8-*I*,*j*)quinolizin-11-one.

Since all the variables except for the HIB layer are fixed, the device performance can be correlated to the type of HIB used and its layer thickness in the OLEDs. The PEDOT layer was deposited by spin coating with a thickness of 40 nm as usual. For P-GO, the layer thickness was controlled to be 1 nm and 2 nm. Since a single-layer P-GO sheet has a thickness between 0.8 and 1.2 nm or an average of ~1 nm, the 1 nm or 2 nm thick HIB layer in the device corresponds to one layer or two layers of P-GO sheets, respectively. It should also be noted that the in-plane gaps and stacks between the P-GO sheets deposited on the electrode depend on the solubility of each of P-GO samples and its concentration in DMF, which in turn can affect the device performance (Fig. 3). Under the same deposition conditions, the saturated DMF solution of sample C led to a film consisting of stacked P-GO sheets without any gaps (Fig. S7 in the ESI†).

The characteristics of the device with P-GO (sample B) are shown in Fig. 4, and the characteristics of all the devices are summarized in Table 1. The devices with 1 nm (round symbols) and 2 nm (triangle symbols) P-GO layers (sample B) work noticeably better than the one with PEDOT (square symbols) in terms of operating voltage, current efficiency and power efficiency (Fig. 4). The improvement in the device performance can be attributed to the unique hole-transport and electron-blocking properties of single-layer, large-area P-GO sheets having an

Table 1 Characteristics of the OLEDs using PEDOT or P-GO

Device	HIB layer	Thickness	Operating voltage/V	Current efficiency/cd A ⁻¹	Power efficiency/lm W ⁻¹
1	P-GO ^a	1 nm	8.1–8.3	21	6
		2 nm	7.7–7.9	23	6
2	P-GO ^b	1 nm	2.5–2.7	23	14
		2 nm	2.6–2.8	20	13
3	P-GO ^c	1 nm	4.3–4.5	20	11
4	PEDOT	40 nm	2.8–3.0	15	11

^a Sample and concentration of P-GO (in DMF): sample A, 0.6 mg mL⁻¹.

^b Sample and concentration of P-GO (in DMF): sample B, 1.0 mg mL⁻¹.

^c Sample and concentration of P-GO (in DMF): sample C, 1.8 mg mL⁻¹.

adequate degree of surface grafting and the use of water-free organic solvent in the fabrication process. For the effect of P-GO thickness, the operating voltage increased and both current and power efficiency went down for the device with a 2 nm thick HIB layer in comparison with 1 nm thickness of P-GO (Table 1). The increase in operating voltage is due to an increase in serial resistance caused by an increase in thickness, which has been observed and explained before.¹⁵ The solubility or degree of surface grafting of P-GO is another factor that can affect the device performance, due to the arrangement of and space between P-GO sheets. For P-GO sample B, there are some overlaps and small gaps as seen in Fig. 3, which would allow efficient hole hopping through and between P-GO sheets. However, for sample A with a lower solubility (0.6 mg mL⁻¹), the P-GO sheets are deposited too much apart; while the P-GO sheets are mostly stacked for sample C with a higher solubility (1.8 mg mL⁻¹) (Fig. S7 in the ESI†). The large gaps between the P-GO sheets on the ITO electrode make hole injection/transport less efficient and more ITO defect sites left uncovered; while the sheet stacking is likely to increase the resistance, which will adversely affect the device performance. Evidently, using P-GO sample A as a HIB, the device with a 2 nm thick P-GO layer performs better than the one with a 1 nm thick P-GO layer, because the 2 nm thick layer consists of two layers of P-GO sheets and has fewer gaps.

4. Conclusions

In summary, we have used a simple surface-grafting method for the preparation of the organo-soluble all-single-layer graphene oxide. With a high solubility in organic solvent, the modified GO is able to form single-layer large sheets that can either be used as an alternative hole-injecting buffer to PEDOT:PSS in optoelectronic devices or as a precursor to single-layer graphene. The OLED device having a single-layer graphene oxide performs better than the one with PEDOT.

Acknowledgements

This work was supported by the National Natural Science Foundation of China (21074132, 20920102032 and 20834001).

Notes and references

- 1 D. J. Milliron, I. G. Hill, C. Shen, A. Kahn and J. Schwartz, *J. Appl. Phys.*, 2000, **87**, 572.
- 2 K. Walzer, B. Maennig, M. Pfeiffer and K. Leo, *Chem. Rev.*, 2007, **107**, 1233.
- 3 N. Koch, S. Duhm, J. P. Rabe, A. Vollmer and R. L. Johnson, *Phys. Rev. Lett.*, 2005, **95**, 237601.
- 4 J. C. Scott, S. A. Carter, S. Karg and M. Angelopoulos, *Synth. Met.*, 1997, **85**, 1197; Y. Zhang, F. He, G. Cheng, C. Ruan, Y. Lin, Y. Zhao, Y. Ma and S. Liu, *Semicond. Sci. Technol.*, 2007, **22**, 214.
- 5 J. Wu, J. Hou, Y. Cheng, Z. Xie and L. Wang, *Semicond. Sci. Technol.*, 2007, **22**, 824.
- 6 H. You, Y. Dai, Z. Zhang and D. Ma, *J. Appl. Phys.*, 2007, **101**, 026105.
- 7 J. Meyer, S. Hamwi, T. Bülow, H. H. Johannes, T. Riedl and W. Kowalsky, *Appl. Phys. Lett.*, 2007, **91**, 113506.
- 8 W. Hu and M. Matsumura, *Appl. Phys. Lett.*, 2002, **81**, 806.
- 9 I. M. Chan and F. C. Hong, *Thin Solid Films*, 2004, **450**, 304.
- 10 D. Zhang, J. Feng, Y. Liu, Y. Zhong, Y. Bai, Y. Jin, G. Xie, Q. Xue, Y. Zhao, S. Liu and H. Sun, *Appl. Phys. Lett.*, 2009, **94**, 223306.
- 11 S. Stankovich, D. A. Dikin, R. D. Piner, K. A. Kohlhaas, A. Kleinhammes, Y. Jia, Y. Wu, S. T. Nguyen and R. S. Ruoff, *Carbon*, 2007, **45**, 1558.
- 12 A. B. Bourlinos, D. Gournis, D. Petridis, T. Szabó, A. Szeri and I. Dékány, *Langmuir*, 2003, **19**, 6050.
- 13 M. J. McAllister, J. Li, D. H. Adamson, H. C. Schniepp, A. A. Abdala, J. Liu, M. Herrera-Alonso, D. L. Milius, R. Car, R. K. Prud'homme and I. A. Aksay, *Chem. Mater.*, 2007, **19**, 4396.
- 14 H. C. Schniepp, J. Li, M. J. McAllister, H. Sai, M. Herrera-Alonso, D. H. Adamson, R. K. Prud'homme, R. Car, D. A. Saville and I. A. Aksay, *J. Phys. Chem. B*, 2006, **110**, 8535.
- 15 S. Li, K. Tu, C. Lin, C. Chen and M. Chhowalla, *ACS Nano*, 2010, **4**, 3169.
- 16 A. A. Green and M. C. Hersam, *J. Phys. Chem. Lett.*, 2010, **1**, 544.
- 17 Y. Zhang, T. Tang, C. Girit, Z. Hao, M. C. Martin, A. Zettl, M. F. Crommie, Y. Ron Shen and F. Wang, *Nature*, 2009, **459**, 820.
- 18 M. F. Craciun, S. Russo, M. Yamamoto, J. B. Oostinga, A. F. Morpurgo and S. Tarucha, *Nat. Nanotechnol.*, 2009, **4**, 383.
- 19 M. Ito, T. Wei, P. Chen, H. Akiyama, M. Matsumoto, K. Tamada and Y. Yamamoto, *J. Mater. Chem.*, 2005, **15**, 478.
- 20 A. Loupya, J. Sansouleta, E. Dez-Barrab and J. R. Carrillo, *Synth. Commun.*, 1991, **21**, 1465.
- 21 P. Šimůnek, A. Lyčka and V. Macháček, *Eur. J. Org. Chem.*, 2002, 2764.
- 22 J. L. Bahr, J. Yang, D. V. Kosynkin, M. J. Bronikowski, R. E. Smalley and J. M. Tour, *J. Am. Chem. Soc.*, 2001, **123**, 6536.
- 23 W. S. Hummers and R. E. Offeman, *J. Am. Chem. Soc.*, 1958, **80**, 1339.
- 24 J. R. Lomeda, C. D. Doyle, D. V. Kosynkin, W. Hwang and J. M. Tour, *J. Am. Chem. Soc.*, 2008, **130**, 16201.
- 25 Z. Sun, S. Kohama, Z. Zhang, J. R. Lomeda and J. M. Tour, *Nano Res.*, 2010, **3**, 117.
- 26 E. Bekyarova, M. E. Itkis, P. Ramesh, C. Berger, M. Sprinkle, W. A. de Heer and R. C. Haddon, *J. Am. Chem. Soc.*, 2009, **131**, 1336.
- 27 M. Fang, K. Wang, H. Lu, Y. Yang and S. Nutt, *J. Mater. Chem.*, 2009, **19**, 7098.
- 28 Y. Li and Y. Wu, *J. Am. Chem. Soc.*, 2009, **131**, 5851.
- 29 X. Wang, S. M. Tabakman and H. Dai, *J. Am. Chem. Soc.*, 2008, **130**, 8152.
- 30 Q. Wang and M. C. Hersam, *Nat. Chem.*, 2009, **1**, 206.
- 31 Z. Sun, S. Kohama, Z. Zhang, J. R. Lomeda and J. M. Tour, *Nano Res.*, 2010, **3**, 117.
- 32 A. Sinitskii, A. Dimiev, D. A. Corley, A. A. Fursina, D. V. Kosynkin and J. M. Tour, *ACS Nano*, 2010, **4**, 1949.
- 33 S. Stankovich, D. A. Dikina, R. D. Piner, K. A. Kohlhaasa, A. Kleinhammes, Y. Jiac, Y. Wuc, S. T. Nguyenb and R. S. Ruoff, *Carbon*, 2007, **45**, 1558.
- 34 K. Haubner, J. Murawski, P. Olk, L. M. Eng, C. Ziegler, B. Adolph and E. Jaehne, *ChemPhysChem*, 2010, **11**, 2131.
- 35 Y. Wang, Z. Ni, T. Yu, Z. X. Shen, H. Wang, Y. Wu, W. Chen and A. T. S. Wee, *J. Phys. Chem. C*, 2008, **112**, 10637.
- 36 D. Abdula, T. Ozel, K. Kang, D. G. Cahill and M. Shim, *J. Phys. Chem. C*, 2008, **112**, 20131.
- 37 K. N. Kudin, B. Ozbas, H. C. Schniepp, R. K. Prud'homme, I. A. Aksay and R. Car, *Nano Lett.*, 2008, **8**, 36.
- 38 X. Ling, L. Xie, Y. Fang, H. Xu, H. Zhang, J. Kong, M. S. Dresselhaus, J. Zhang and Z. Liu, *Nano Lett.*, 2010, **10**, 553.
- 39 S. Park, J. An, R. D. Piner, I. Jung, D. Yang, A. Velamakanni, S. T. Nguyen and R. S. Ruoff, *Chem. Mater.*, 2008, **20**, 6592.
- 40 D. Graf, F. Molitor, K. Ensslin, C. Stampfer, A. Jungen, C. Hierold and L. Wirtz, *Nano Lett.*, 2007, **7**, 238.
- 41 S. Park and R. S. Ruoff, *Nat. Nanotechnol.*, 2009, **4**, 217.
- 42 X. Wang, S. M. Tabakman and H. Dai, *J. Am. Chem. Soc.*, 2008, **130**, 8152.